CrossMark

REVIEW ARTICLE

Fuzzy gamma operator model for preparing landslide susceptibility zonation mapping in parts of Kohima Town, Nagaland, India

Hinotoli V. Sema[1] · Balamurugan Guru[1] · Ramesh Veerappan[1]

Abstract Growing population and expansion of settlements over hilly areas have largely increased the impact of landslide. This paper deals with the use of Geoinformatics technology and Fuzzy Gamma Operator model to map the landslide susceptibility zones in part of Kohima Town, Nagaland. For this study, eight landslide inducing parameters such as slope gradient, slope aspect, curvature, elevation, land use and land cover, drainage density, lineament density, and topographical wetness index were considered and prepared with the help of toposheet, high resolution satellite imagery such as World View II, LISS IV, DEM data and field data. Landslide inventory was the first step for the geospatial database generation which involves the mapping of past landslide details. Landslide susceptibility maps were generated by calculating relationship between the landslide inducing factors with past landslide locations using frequency ratio and fuzzy gamma operator model. The ratios were normalized between the range of 0 and 1 to obtain fuzzy membership values. The landslide susceptibility zonation (LSZ) map were prepared by integrating all the causative factors with fuzzy membership values and classified into five different susceptibility classes based on Jenks natural breaks classification viz. very high (37.51%), high (32.21%), moderate (20.97%), low (7.97%), and very low (1.34%). The LSZ map were compared with the landslide inventory map and validated with best prediction accuracy using area under curve (AUC) with the accuracy level and R-Index.

✉ Balamurugan Guru
gurubala.jtcdm@gmail.com

1 Centre for Geoinformatics, Tata Institute of Social Sciences (TISS), Malti and Jal A. D. Naoroji Campus (Annex), Post Box No: 8313, Deonar Farm Road, Deonar, Mumbai 400088, Maharashtra, India

Introduction

Landslides are one of the most common events in mountainous region because of their physiographic, topographic and other triggering factors like earthquake, rainfall, water level changes, and rapid stream erosion, etc (Dai et al. 2002). Increase in human population and rapid urbanization has also led to expansion of construction activities especially in hilly terrains and has also resulted in frequent landslide occurrences in these regions (Thong et al. 2006; Aier 2005). Landslides pose a serious geological hazard especially in rugged mountainous terrain like the Himalayas, Western Ghats, Eastern Ghats and also Arakan-Yoma ranges. Presence of steep slopes, weak rocks and periodic occurrence of prolonged and intense rainfall, soil type and its thickness, human activities etc. causes major landslide events in many parts of the region (GSI 2001; Husain 2008). Over the years, many people lost their life and large amount of properties have also been lost due to landslide in the region (Alexander 1993).

Preparation of the landslide hazard susceptibility mapping is an essential task for geoscientists, planners and local administrators in globally to minimize the impact from landslide events and also source for decision making and developmental activities in an area (Devoli et al. 2007). Landslide hazard zonation mapping is also an important tool which gives the details about the possible landslide occurrence of a certain type and magnitude in a particular location within a set time (Varnes 1984; Corominas and Moya 2008). The landslide susceptibility zonation mapping

🌐 Springer

500

Model. Earth Syst. Environ. (2017) 3:499–514

preparation techniques includes various approaches and methods such as qualitative, quantitative, distribution free, deterministic (Kanungo et al. 2009). The qualitative approach is subjective where knowledge and experience of experts play significant role to generate landslide mapping (Aleotti and Chowdhury 1999). Whereas in quantitative approach, the relative importance of causative factors were quantified in objective way i.e. on the basis of relationship between past landslide distribution and causative factors (Carrara 1988; Guzzetti et al. 1999). The quantitative analysis encompasses both bivariate methods like frequency ratio (Ayalew et al. 2005; Lee and Pradhan 2006; Yilmaz and Keskin 2009; Ehret et al. 2010; Intarawichian and Dasananda 2011; Kannan et al. 2013; Sujatha et al. 2013), logistic regression (Lee et al. 2002; Akgün and Bulut 2007; Nandi and Shakoor 2008; Tunusluoglu et al. 2008; Sujatha et al. 2011; Xu et al. 2013; Regmi et al. 2014) information value method (Jade and Sarkar 1993; Van Westen 1997; Saha et al. 2005), relative effect models (Naveen Raj et al. 2011; Anbazhagan and Ramesh 2014) and multivariate method like discriminant analysis, regressive multiple analysis (Duman et al. 2006; Das et al. 2012; Regmi et al. 2014; Shirzadi et al. 2012). In the present study, the fuzzy logic approach was applied for the part of Kohima Town, Nagaland. Hence, the steps involved are: (1) prepare a landslide inventory map and maps of causative factors, (2) fuzzy logic to assess the impact of each factor of landslide (3) apply fuzzy operators for combining all fuzzy causative factor to obtain a landslide susceptibility zonation map, and (4) validate the accuracy of the obtained landslide susceptibility zonation map. Geographical information system (GIS) and Remote Sensing act as an important set of tools for collecting, storing, retrieving, transforming and displaying spatial data from the real world for a particular area for landslide susceptibility mapping (Balamurugan et al. 2016). Over the past 3 decades, these tools have been helpful in the assessment of natural as well as man-made disasters.

Study area

The study area is part of Kohima Town which is the capital of Nagaland and situated in the North-eastern part of India (Fig. 1). The study area is part of Kohima Town which is the capital of Nagaland and situated in the North-eastern part of India (Fig. 1). The urban area of this town covers approximately 13.06 km^2 and includes parts of the National Highways (NH) 39 and NH-61 respectively. Kohima Township is divided into 19 wards however, the study area consists of 10 Wards namely New Market Officer's Hill, PWD, Upper Chandmari, Lower Chandmari, Dzuvuru A.G New Minister's

Hill Agri Forest Paramedical (Merhuliesta), P.R Hill and it covers 7.10 km^2. Kohima is well connected with other part of the state by a road networks and the railway station and airport are located at Dimapur which is located at 74 km. The study area is a undulated and rugged terrain and elevation varies from 1250 to 1750 m above mean sea level. The area of study lies in the humid tropical climatic zone and winter falls in December and January months are the coldest part of the year when temperatures fall to 5 °C or less. The summer temperature rises up to 25 °C from April and May months.

Rainfall

The study area receives the rainfall during the monsoon from month of July to August with occasional rainfall from September to October months in every year. Cloudbursts are common phenomena in some part of the state including Kohima. Storms are rare event during certain seasons. In the present study area there is only one rain gauge station situated at Kohima town. The average rainfall of the district is about 2000 mm. The maximum rainfall per day of the study area is measures as 689.4 mm. The average annual rainfall too varies within wide limits. 30 years (from 1985 to 2015) of rainfall data were obtained from Soil and Water Conservation Department, Kohima during the field visit. The maximum rainfall receives in the study area in 1993 as 2616 mm and minimum rainfall receives as 690 mm in 2006 (Fig. 2).

Geological set-up and soil

Kohima Town made up of a young geologic terrain with pervious soils and unstable rocks. Tectonism has caused large scale folding and faulting that has resulted in severe fracturing and crumpling of the rocks. Folding is responsible for the tight anticlines and synclines at places in the rocks of the area which have been further altered by the geomorphic processes. The erosional processes that dissect geologic structures help loosen rock masses on slopes of present topography. Fracture zones and systems of joints and faults display different orientations along slopes and ridges (Walling 2009; Supongtemjen 2006). The soil of the study area belongs to two major groups namely grey clay and red clay soil however; it is not possible to trace the continuity of geology and soil for large distances due to vegetation, and human settlements. This area is made up rocks of the Disang Group dominantly covered by shale at some places, where shale has been changed into slate because of metaphorphism. The Disang are made up of abundant splintery shales with alternations of thin flaggy sandstones. The shales are highly crumpled at places and

Model. Earth Syst. Environ. (2017) 3:499–514

501
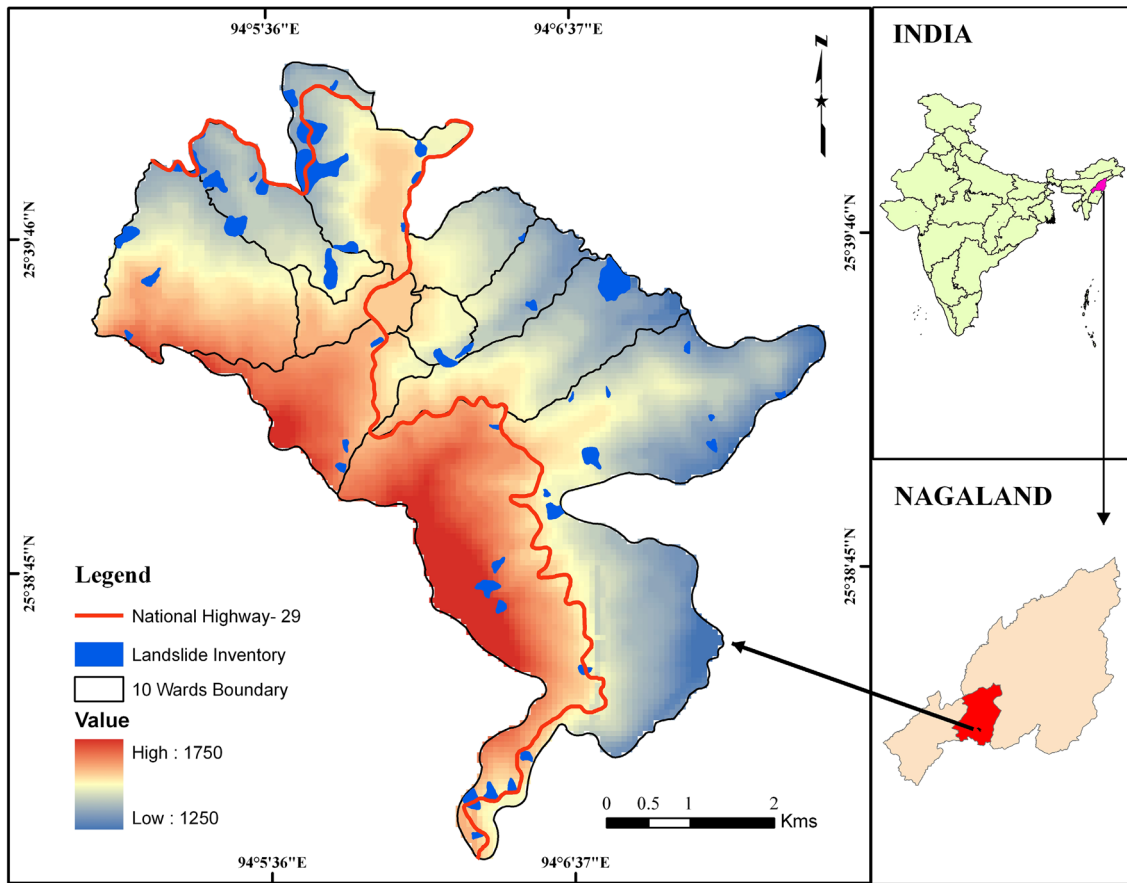
Fig. 1 Location, digital elevation model (DEM) and past landslides of part of Kohima Town

Fig. 2 Rainfall data from 1985 to 2015
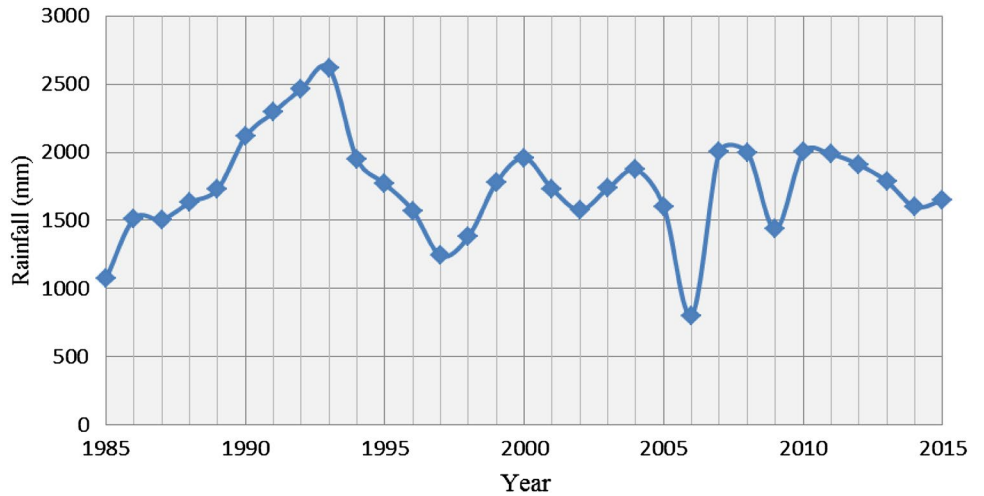
at others they are partially to completely weathered. Landslides frequently occur in the areas made up of the shales (DGM 2009; MWR 2013).

Historical landslides data

Landslide events of Kohima Town are concentrated along the hillside, drainages and steep slopes. Nearly all the landslides, both small and very large landslides, are triggered

502

Model. Earth Syst. Environ. (2017) 3:499–514

by heavy rainfall during monsoon season and also some reported landslides have been caused at least partly by human activities. The historical landslide database was produced from records of various government agencies and also prepared from field visit. In the present study, historical landslides occurrences and its impact is given in Table 1. During the field visit it has been observed that human activities such as unscientific manner of constructing of buildings in the hill slope also caused the landslide (Fig. 3 a–c). Figure 3c shows the landslide event occurred due to improper drainage embankment construction along the slope. Moreover, during the field visit also noticed that some the landslide events were not reported if it did not affected a people or building structures.

Spatial database generation

In this study, characteristics of slope gradient, slope aspect, slope curvature, lithology, land use and land cover, lineament density, drainage density, topographic wetness index (TWI) were considered as landslide influencing factors for thematic map generation. Although most of the landslides were triggered by external factor like rainfall, it is not as thematic factor due to less spatial variation of rainfall because of the smaller area. Also, the study area lies in the high seismic zone V, the seismicity index is not considered for thematic factor.The Survey of India (SOI) topo map, Satellite imagery, and Digital elevation model (DEM) are

the data sources used for the derivation for all the parameters. The DEM was generated using the 25 m interval contours digitized from SOI toposheet. The detailed information of data source is given in Table 2. All the thematic maps were classified and the entire vector format was converted into 10×10 raster grid cell.

Landslide inventory

Landslide inventories are the simplest form of landslide mapping (Guzzetti et al. 1999). It shows the location of landslide occurrences in the form of landslide scars (Van Westen and Terlien 1996; Parise 2001).The inventory map of past landslide locations consists of the information about the existing landslides in an area, which is helpful to validate the landslide susceptibility map and also gives the information of conditions and processes which influence past landslide occurrences and their evidences is the most significant aspect for the prediction of future landslides (Yilmaz et al. 2012). An inventory record also contains the information of landslide locations, types, time and date, areal extension that has left discernible traces in an area. The different techniques used to prepare inventory maps depend on (1) the reason the map is being prepared, (2) the extent of the study area, (3) the scales of base maps and aerial photographs, and (4) the resources available to carry out the work (Guzzetti et al. 1999).

In the present study, 46 landslide locations were identified from the field and based on this information the

Table 1 Historical landslide occurrences and its impact

Sl. no	Years	Incidences	Impacts
1	1934	Keziekie slide	Highway effected for many days
2	1942	Keziekie slide	Highway affected and communication
3	1943	T. C. P. gate	According to the local residents and respondents, the presence of seepage of water present in that area may be the cause of the slide. The seepage is a source of water supply to the surrounding area
4	1962	Midland colony	No damage to property was reported since the areas had no buildings at that time. However, there were some paddy fields washed away by landslides
5	1976	Keziekie slide	Houses, Vegetation was destroyed
6	9th August 2001	Kohima town	200 houses damaged, 500 people died, about 5 km road damaged
7	2003	Lerie slide	Affected communication and transportation disrupted for many days
8	2003	Paramedical slide	NH 39 and houses damaged
9	2003	Midland slide	Footpaths connecting the two colonies are constantly destroyed. Small bridges connect the two sides over the two small streams
10	2003	Chiepfütsiepfe slide	Road was totally damaged up to a length of 73 m
11	August 2003	Kohima town	Many houses were razed to ground and many more were made unfit fot habitation. The road was badly affected and that for a year it had to be abandoned. Properties worth lakhs were destroyed by this slide
12	17th October 2007	National highway 39 near Kiruphema	About 150 m of National Highway 39 near Kiruphema went down almost 400 m. This resulted in the complete blockade of the highway for 2 days

Source: Directorate of Geology Mining (2009); Data from field visit in 2014

Fig. 3 Pre and post landslide location of the study area; location D block **a** pre landslide taken on 4th June 2014 and **a1** post landslides taken on 26th August 2014, **b** and **c** landslide locations in Agri/Forest and paramedical respectively

Table 2 Detail of thematic data layers and data sources

Types of thematic data layers	Sub classification	Data types in GIS	Scale/ Resolution	Source
Landslide inventory	–	Polygon	–	World view II (0.5 m) LISS4 (5.8 m)
Topographic maps	Slope gradient	Grid	10×10 m	DEM (Toposheet, SOI at 1:25,0000 scale)
	Slope aspect	Grid	10×10 m	
	Slope curvature	Grid	10×10 m	
	Topographic wetness index	Grid	10×10 m	
Geological map	Lithology	Polygon	–	Geological map, GOI (1:50,000)
Lineament	Lineament density	Grid	10×10 m	LISS4 (5.8 m)
Drainage map	Drainage density	Grid	10×10 m	Toposheet, SOI(1:25,0000)
Land cover	Land use land cover	Polygon	–	LISS4 (5.8 m)

504

Model. Earth Syst. Environ. (2017) 3:499–514

inventory data has been created with respective geographical locations in GIS data base. A characteristic of historical landslide inventories is that evidence of the existence of landslide occurrences however, many of smaller scale landslides has been lost due to various degrees of modification by subsequent landslides, erosional processes, anthropic influences, and vegetation growth. On the other hand there is an accumulating evidence that in many historical landslide inventories, the frequency, and the coverage area distribution of medium to large landslides decays due to landslide controlling structures in the landslide affected areas (Sasaki et al. 1991; Dai and Lee, 2001; Guzzetti et al. 2002; Dussauge et al. 2002; Dussauge et al. 2003.

Terrain parameters

The important characteristics of landslides in the study area consist of a multiple sets such as lithology, slope stability and also high intensity of rainfall. The parameters responsible for landslides activity includes slope gradient, slope aspects, slope curvature, land use and land cover, vegetation cover, elevation, drainage, lineament and TWI. The important landslide induced terrain parameters of the study were extracted from remotely sensed data, toposheet, digital elevation model and field data. Topographic parameters such as slope gradient and slope aspect play a crucial role in steep mountainous terrain for influencing mass movement process (Guzzetti et al. 2012).

DEM

A Digital Elevation Model (DEM) represents spatial variation in altitude. DEM was prepared by digitizing the detailed topographic map with the contour interval of 25 m. DEM was used to generate different thematic maps such as slope gradient, slope aspect, slope curvature and elevation map. It is the first derivative of elevation with each pixel denoting the angle of slope at a particular location. It is the most important inherent factors of landslide.

Slope gradient

Slope is the angle between the surface of earth and a horizontal datum. It is an important parameter in landslide analysis. Slope map layer contains slope values, stated in degrees of inclination from the horizontal. The flat slope angle is safer in terms of failure initiation as compared to steeper slope. In the study area the slope gradient is classified into five classes ranging from 0°–8°, 8°–14°, 14°–20°, 20°–27°, and 27°–49° (Fig. 4a).

Slope aspect

Slope aspect describes the direction of slope terrain. Aspect shows a strong inheritance from bedrock structure and influences the exposition to sun and thereby changes in vegetation and evapo-transpiration (Fernandez Merodo et al. 2004; Balamurugan and Ramasamy 2006). The slope aspect is divided into eight directional classes such as flat, north, north east, east, south, south east, south west, west, and north west (Fig. 4b).

Slope curvature

Curvature is defined as the curvature of a line formed by intersection of a random plane with the surface (Duman et al. 2006; Ramani et al. 2011). In the present study, the curvature map is divided into three classes where the negative values were classified as concave, the positive values as convex, and zero values classified as flat as shown in Fig. 4c.

Topographic wetness index (TWI)

Topographic wetness index is the steady state wetness index (Beven and Kirkby 1979). It indicates the saturated source zone due to surface run off under the influence of topography condition. Mathematically it is denoted as follows (Eq. 1).

$$TWI = In\left(\frac{As}{\tan \beta}\right), \tag{1}$$

where As is the cumulative upslope area draining through a certain point (per unit contour length) and β is the slope gradient in degree.

Hence, topographic Wetness index has positive correlation with the infiltration of rainfall into slope forming materials which increases pore pressure of the slope (Yilmaz and Keskin 2009). In this study TWI was prepared from DEM by topographic wetness tool in SAGA GIS. The whole map was classified into five classes viz. 1.199367046–6.178712368, 6.178712369–9.073779106, 9.073779107–12.12327671, 12.12327672–14.69011593 and 14.69011594–18.99362946 following natural breaks method (Fig. 4d).

Land use and Land cover

The land use land cover map was interpreted using high resolution satellite images. The study area was classified into four different land use and land cover pattern such

Model. Earth Syst. Environ. (2017) 3:499–514

505
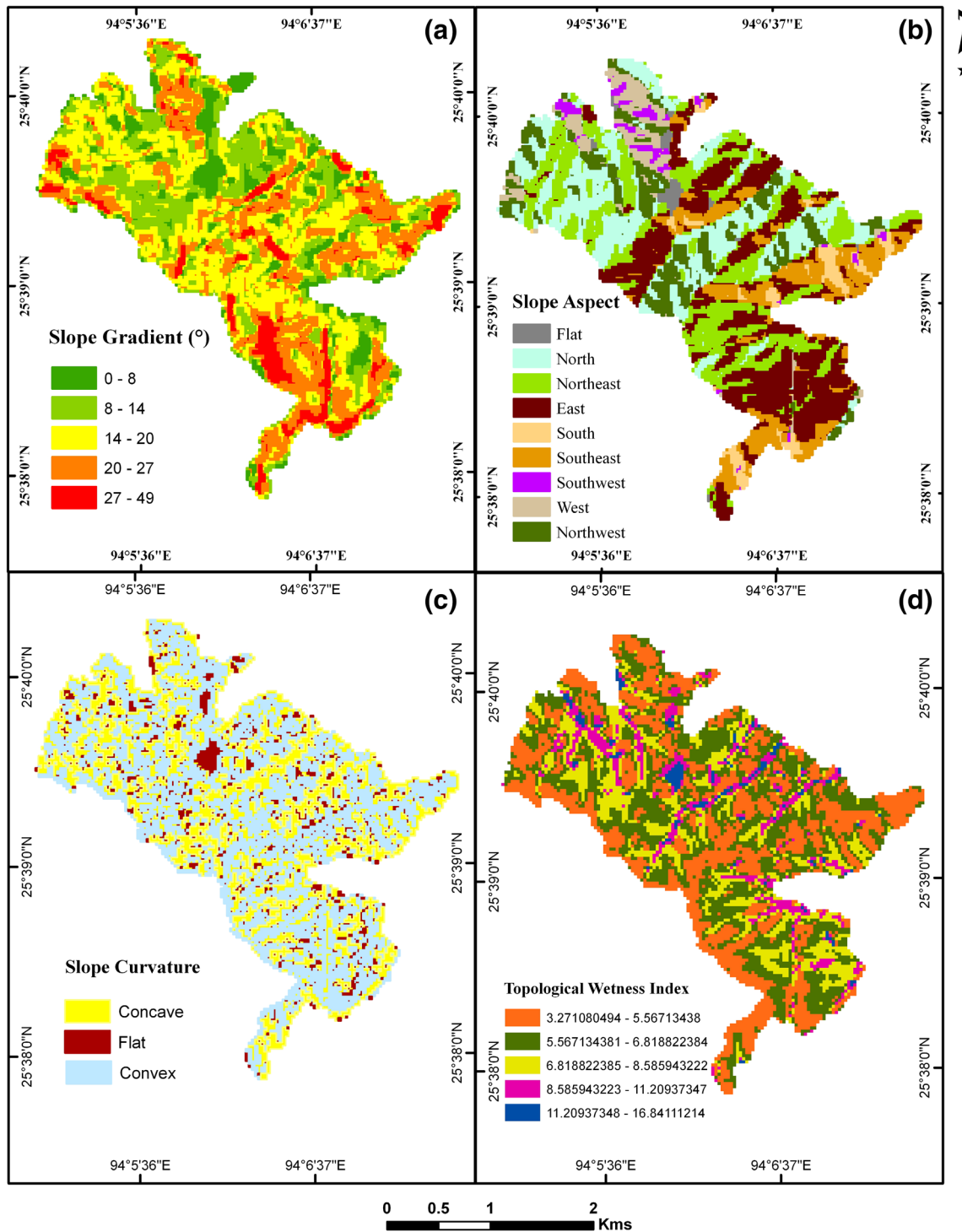
Fig. 4 Thematic maps of causative factors—**a** slope gradient, **b** slope aspect, **c** slope curvature, **d** topographic wetness index

as mixed built-up area, forest, cultivation and scrub and bushes. The study area is dominated by Mixed-built since it is an urban area (Fig. 5a).

Elevation

Generally, elevation of an area affects the biophysical parameters, anthropogenic activities and rock

506

Model. Earth Syst. Environ. (2017) 3:499–514
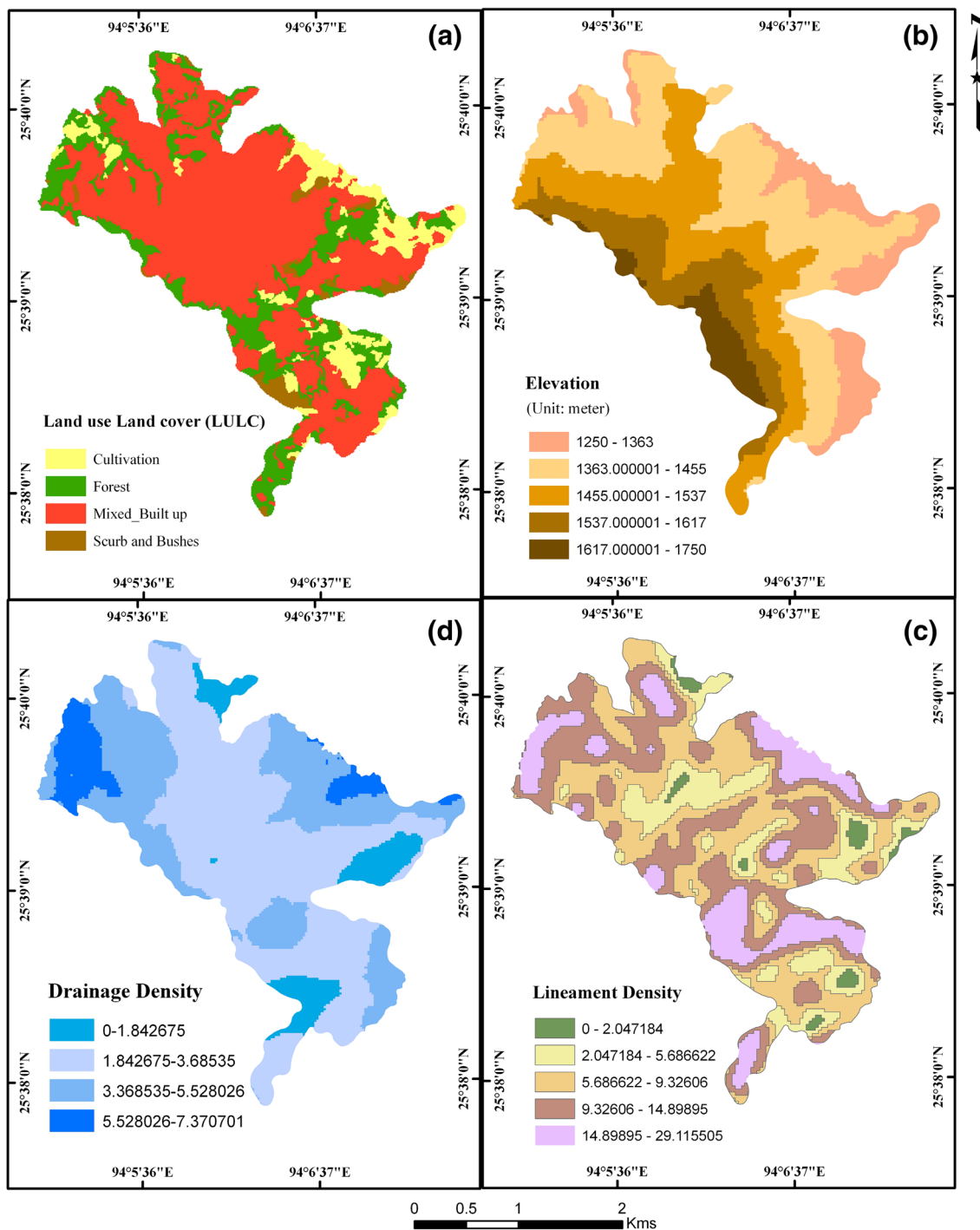
Fig. 5 Thematic maps of causative factors—**a** land use and land cover, **b** elevation, **c** lineament density and **d** drainage density

characteristics. The highest elevation of the Township is 1750 m and the lowest elevation is 1250 m. On the basis of Jenks natural breaks classification (Jenks 1967), the elevation range was classified into five classes viz., 1250–1369, 1369–1439, 1439–1515, 1515–1603 and 1603–1750 as (Fig. 5b).

Lineament density

Lineaments features area representing the faults, fractures, shear zones, etc., are the most obvious structural interpretations on the satellite imagery (Srileka 2014). Hence, the probability of landslides occurrences increases with increase in closeness of lineaments (Kannan et al. 2013;

Pradhan et al. 2009). The lineament map shows the lineaments formed in the study area due to the geological conditions (Balamurugan and Ramasamy 2006; Pattusamy and Purusothaman 2014). The lineaments were interpreted from LISS IV image by adopting different digital image processing techniques such as edge–enhancement, and contrast stretching. The lineament density was calculated by the total length (m) of lineament per grid and the value was converted and prepared by Euclidean distance method it was classified into five classes i.e. 0–2.047184 m, 2.047184–5.686622 m, 5.686622–9.32606 m, 9.32606–14.89895 m, 14.89895–29.115505 m (Fig. 5c) by natural breaks method.

Drainage density

Drainage density is the ratio of total length of a stream to the area of the drainage basin; the higher the drainage density, the lower the infiltration and the faster the movement of surface flow (Pachauri et al. 1998; Nagarajan et al. 2000). Drainages describe the activity of erosion and morphological changes in hilly region. The presence of drainages close the landslide location influences more comparatively which is located further away (Barrendo et al. 2000; Srivastava et al. 2010). Drainage density, total stream length per unit area represents the degree of fluvial dissection. The drainages were digitized from Toposheet map of the year 2005 on 1:5000 scale and updated with recent satellite images. The proximity to drainage was calculated by line density method in ArcMap 10@ESRI and classified into four classes viz. 0–1.842675 m, 1.842675–3.68535 m, 3.368535–5.528026 m, 5.528026–7.370701 m, by following natural breaks method (Fig. 5d).

Methods—fuzzy gamma operator model

Zadeh (1965) was the first to introduce the fuzzy set theory to analyse mathematically non-discrete natural processes or phenomena. A fuzzy set is a class of objects with a continuum of grades of membership, characterized by a membership function which assigns to each object a grade of membership ranging between zero and one (Zimmermann 1996). In fuzzy set theory, membership values were assigned in between 0 and 1 reflecting the degree of certainty of influencing factor in landslide susceptibility. The membership values 1 and 0 contribute the maximum and minimum or nil influence of landslide susceptibility of a particular influencing factor respectively. In landslides susceptibility mapping, all the classes of the nine thematic causative factors are considered as a member in the set of landslide susceptibility area. The fuzzy membership

value can be derived from different method like normalization of frequency ratio (Lee 2007; Pradhan et al. 2009; Ramesh and Anbazhagan 2015; Kumar and Anbalagan 2015; Balamurugan et al. 2016) and information value (Yin and Yan 1988), the cosine amplitude method (Ercanoglu and Gokceoglu 2004; Kanungo et al. 2006), or subjective based (Bonham-Carter 1994; Tangestani 2004; Champatiray et al. 2007; Ray et al. 2007). Different operators can be employed to combine the membership values when two or more thematic maps with fuzzy membership functions. Cascini et al. 1991, discussed five operators, namely the fuzzy AND, fuzzy OR, fuzzy algebraic product, fuzzy algebraic sum and fuzzy gamma operator. This study uses the fuzzy algebraic sum, the fuzzy algebraic product, and fuzzy gamma operator for combining the fuzzy membership functions.

In the present study, fuzzy gamma operator was used to prepare landslide susceptibility map and the fuzzy membership values were derived from frequency ratio values. However, the value of 0.0001 have assigned for zero membership value case to avoid the complete omission of a class in a causative factor for landslide hazard zonation analysis (Srivastava et al. 2010). The frequency ratio values were determined by relating the existing landslides with each causative factors using Eq. 2.

$$FR = (Li/Lt)/(Fi/Ft), \tag{2}$$

where Li number of landslide pixel in class 'I' of a factor, Lt total number of landslide pixel within study region, Fi number of pixel in each classes of thematic factor, Ft total number of pixel in all classes of the thematic factor, FR frequency ratio.

Then fuzzy membership value was calculated by normalizing the value of frequency ratio following Eq. 3.

$$(X_{FR} - MIN_{FR})/(MAX_{FR} - MIN_{FR}) \tag{3}$$

The fuzzy algebraic product and fuzzy algebraic sum were calculated using Eqs. 4 and 5.

$$\mu_{combination} = \prod_{i=1}^{n} \mu i, \tag{4}$$

$$\mu_{combination} = 1 - \prod_{i=1}^{n} (1 - \mu i), \tag{5}$$

where μi is the fuzzy membership function for the ith parameter, and $i = 1, 2 \cdots n$ parameter are to be combined.

The fuzzy Gamma Operator was calculated by following Eq. 6. Where, the value γ should be ranged between 0 and 1.

$$\mu_{combination} = (Fuzzy\,a\lg ebraic\,sum)^{\gamma} \\ \times (Fuzzy\,a\lg ebraic\,product)^{1-\gamma}, \tag{6}$$

508

Model. Earth Syst. Environ. (2017) 3:499–514

Kannan et al. (2013) used R-index for validation for hazard zonation. It illustrates the performance of hazard classification. Symbolically it can be denoted as–

$$R = \frac{x_i/X_i}{\sum(x_i/X_i)} \times 100 \qquad (7)$$

x_i is the number of landslides in hazard class 'i' and X_i is the number of total pixel in the same class 'i'.

Results and discussion

The eight causative factors (slope gradient, slope aspect, curvature, elevation, land use and land cover, drainage density, lineament density and topographical wetness index) were combined to create a landslide susceptibility index map using the frequency ratio and fuzzy operators. The frequency ratio (FR) values were calculated using Eq. (2) for each class present in all the nine causative parameter maps based on the relationship with the landslide inventory dataset. The fuzzy membership values were normalized from frequency ratio values between 0 and 1 (Table 3). The relationship results in weights, which can directly be evidence for the influence of each class in a causative factor for the landslide susceptibility. The slope gradient ranging from 25.88894116°–56.26529876° areas having the highest value of 1.67, reveals the highest probabilities of landslide occurrences in the study area. The west-facing and southwest-facing slopes are more susceptible to failure. The convex and concave slope possesses 43.22 and 48.64% landslide pixels, respectively, whereas the flat slope has 8.14% of landslide pixels. The analysis also points out that landslide are more abundant in the elevations between 1363–1455 m with 36.52%. Among different land use land cover class present in the study area, the Mixed-Built up shows a high probability and has the number of landslide of 1117 pixels followed by forest having the value of 974 pixels. The relationship between past landslides and drainage density ranges between 0.64 and 1.16. The value of frequency ratio for lineament density ranges from 0.33 to 1.73.

Landslide susceptibility mapping

The landslide susceptibility mapping was prepared on the basis of Fuzzy Gamma Operator. All the eight thematic map of causative factors and landslide inventory map were converted into raster file with 10-m grid for integration in GIS platform. The total number of landslides in the study area is 46 and it occupied 2702 pixels. The study area covers total 71,040 numbers of pixels. Landslide susceptibility index (LSI) was derived by integration in GIS platform

following Eq. 6 for FGO. The higher value of LSI indicates higher susceptibility of landslide; in opposite lower value of LSI indicate lower susceptibility of landslide. In the case of FGO model, the different landslide susceptibility map were prepared and tested on the basis of different γ value which was ranged from 0.2 to 0.975. It was seen that γ value of 0.975 brought better accuracy in validation than other γ value. So, 0.975 was considered as final input γ value for landslide susceptibility mapping.

The percentage of landslide frequency in susceptibility classes were derived by overlying of landslide inventory map on landslide susceptibility map. In FGO model, maximum and minimum value of LSI is 0.976679206 and 0.234069407. The range of LSI value is classified by natural breaks method into five classes viz; 1.67% (very low), 7.88% (low), 21.35% (moderate), 45.63% (high), and 23.46% (very high) of total study area (Fig. 6). The percentage of landslide frequency in susceptibility classes were derived by overlying of landslide inventory map on landslide susceptibility map. It is shown about from the above classification that 69.10% of landslide is concentrated in high and very high susceptibility class of FGO model (Fig. 7; Table 4).

Validation

Validation is the finally and most important step for assessment of accuracy level of any model. The landslide susceptibility model of the FGO was validated using area under curve (AUC) method and R-Index using Eq. 7. AUC is used to assess the prediction accuracy of any model qualitatively (Begueria 2006; Pradhan and Lee 2010). AUC value is ranged from 0.5 to 1 in which 0.5 indicates an ideal lowest inaccuracy rate and 1 indicates an ideal highest accuracy rate of any model (Nandi and Shakoor 2010). In AUC method success rate curve shows accuracy rate of model graphically. The AUC was derived on the basis of relationship between cumulative percentage of landslide occurrence and LSI value. In this regard, LSI was snumber of landslides in hazard classshorted in descending order and reclassified into 100 classes to evaluate cumulative frequency of landslide occurrence in each class. In the present study the AUC value of FGO is 0.64 (Fig. 8). It indicates the accuracy level of landslide susceptibility zonation for FGO method is 64.33% and R-index value increase from 21.03301(very low) to 248.9346 (very high) which is represented graphically in the Fig. 9.

Conclusion

With the advancement of Remote Sensing and GIS, a great deal of help can be had in the planning and implementation

Table 3 Frequency Ratio and Fuzzy Membership value of classes of influencing factors of slope gradient, slope aspect, curvature, elevation, land use land cover, drainage density, lineament density and TWI

| Influencing factor	Class	No. of pixels in domain	% of pixels in domain	No. of landslide in domain	% of landslide in domain	Frequency ratio	Fuzzy membership values
Slope gradient	0–4	3608	5.08	71	2.63	0.52	0.0001
	4.487416467–12.08150587	12,396	17.45	498	18.42	1.06	0.47
	12.08150588–18.64003763	25,100	35.33	693	25.64	0.73	0.18
	18.64003764–25.88894115	22,272	31.35	955	35.33	1.13	0.53
	25.88894116–56.26529876	7664	10.79	486	17.98	1.67	1
Slope aspect	Flat (−1)	900	1.27	3	0.11	0.09	0
	North (337.5–22.5)	14,417	20.29	451	16.69	0.82	0.27
	Northeast (22.5–67.5)	15,074	21.22	567	20.98	0.99	0.33
	East (67.5–112.5)	17,303	24.36	583	21.57	0.89	0.29
	Southeast (112.5–157.5)	8182	11.52	182	6.73	0.58	0.18
	South (157.5–202.5)	2475	3.48	57	2.11	0.61	0.19
	Southwest (202.5–247.5)	1637	2.30	177	6.55	2.84	1
	West (247.5–292.5)	3436	4.84	364	13.47	2.78	0.98
	Northwest (292.5-337.5)	7616	10.72	319	11.80	1.10	0.37
Curvature	Concave (−)	30,703	43.22	1464	54.16	1.25	1
	Flat (0)	5780	8.14	139	5.14	0.63	0
	Convex (+)	34,557	48.64	1100	40.70	0.84	0.34
Elevation	1250–1363	10,259	14.44	843	31.19	2.16	1
	1363.000001–1455	25,944	36.52	1145	42.36	1.16	0.47
	1455.000001–1537	20,252	28.51	495	18.31	0.64	0.19
	1537.000001–1617	10,544	14.84	115	4.25	0.29	0
	1617.000001–1750	4041	5.69	105	3.88	0.68	0.21
Land use and land cover	Forest	15,434	21.73	974	36.03	1.66	0.96
	Cultivation	7641	10.76	456	16.87	1.57	0.88
	Mixed-built up	45,549	64.12	1117	41.32	0.64	0
	Scrub and bushes	2416	3.40	156	5.77	1.70	1
Density drainage	0–1.842675	5725	8.06	147	5.44	0.67	0.06
	1.842675–3.68535	37,170	52.32	1423	52.65	1.01	0.71
	3.368535–5.528026	22,724	31.99	1000	37.00	1.16	1
	5.528026–7.370701	5421	7.63	133	4.92	0.64	0
Density lineament	0–2.047184	1678	2.36	24	0.89	0.38	0.04
	2.047184–5.686622	11,528	16.23	144	5.33	0.33	0
	5.686622–9.32606	23,986	33.76	445	16.46	0.49	0.11
	9.32606–14.89895	21,634	30.45	1287	47.61	1.56	0.88
	14.89895–29.115505	12,214	17.19	803	29.71	1.73	1
Topographical wetness index (TWI)	1.199367046–6.178712368	37,836	53.26	1314	48.61	0.91	0
	6.178712369–9.073779106	26,774	37.69	958	35.44	0.94	0.01
	9.073779107–12.12327671	5292	7.45	336	12.43	1.67	0.37
	12.12327672–14.69011593	753	1.06	52	1.92	1.81	0.44
	14.69011594–18.99362946	385	0.54	43	1.59	2.94	1
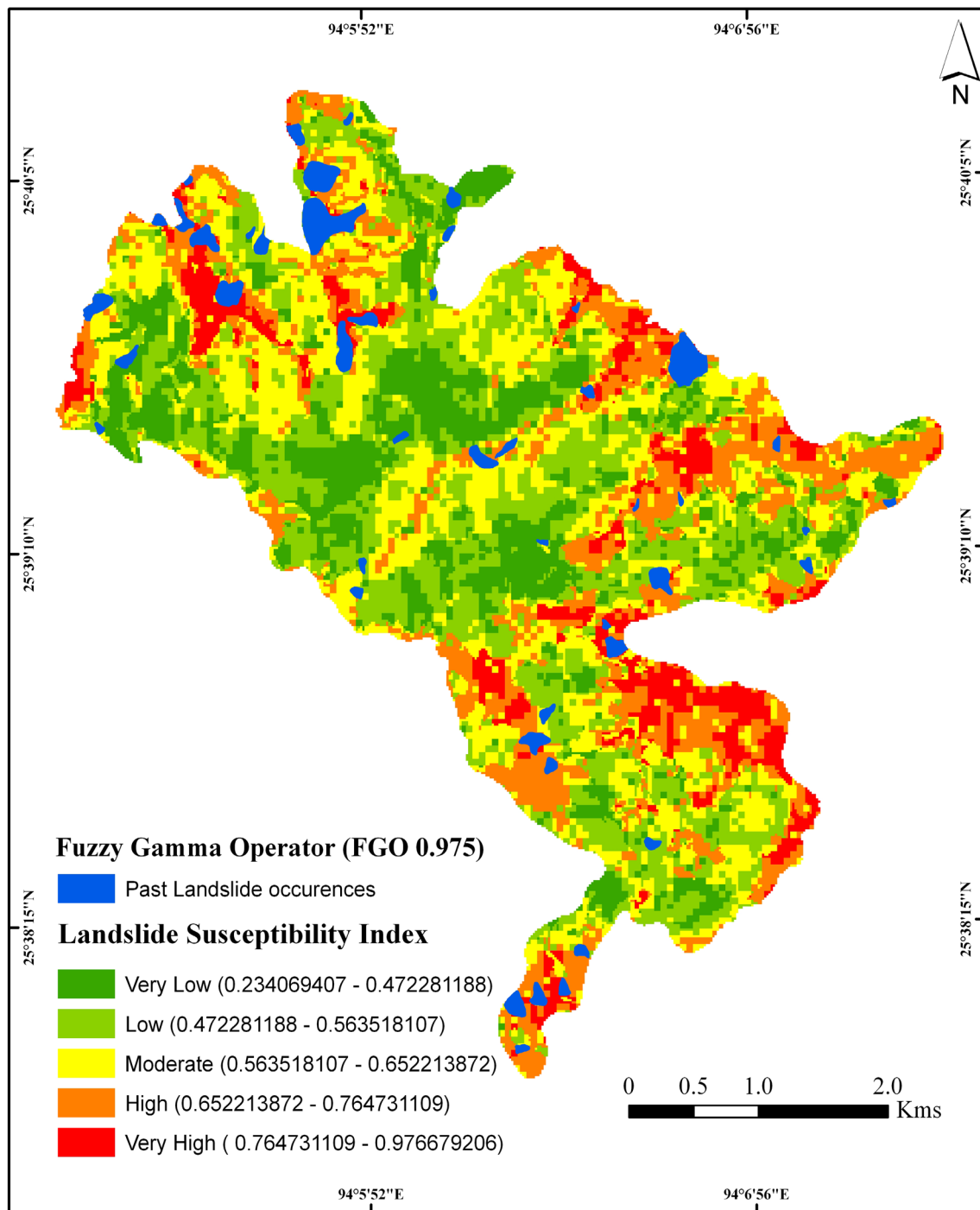
Fig. 6 Landslide susceptibility zonation map using fuzzy gamma operator (FGO) model

of disaster risk reduction measures. Data collection, manipulation and the analysis of the necessary environmental data is an important step for landslide susceptibility analysis (Carrara 1988). Unlike other methodologies to assess landslide susceptibility, the fuzzy logic approach fuzzy gamma operator and γ values for the fuzzy γ operation was used to prepared landslide susceptibility maps

in part of Kohima Town, Nagaland. By using the fuzzy logic approach, landslide susceptibility analysis was done by having few existing data about the factors causing the landslides. The fuzzy operator producing the best success rate accuracy which can be identified based on success rate curves and R-index curves so as to generate the most accurate landslide susceptibility zonation map. The landslide

Fig. 7 Landslide frequencies in each class of landslide susceptibility model
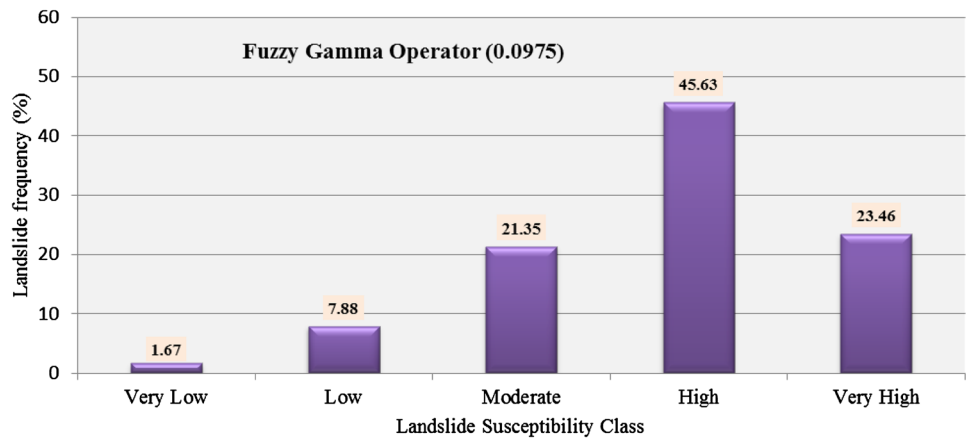

Table 4 No and percentage of pixel in each class of landslide susceptibility index by FGO method

Methods of LSI	Classes of LSI	No. of pixel in classes	% of pixel in classes	No. of landslide pixel in classes	% of landslide pixel in classes
FGO (0.975)	Very low	5625	7.92	45	1.67
	Low	17,302	24.36	213	7.88
	Moderate	24,907	35.06	577	21.35
	High	16,509	23.24	1233	45.63
	very high	6096	9.43	634	23.46

LSI landslide susceptibility index, *FGO* fuzzy gamma operator

Fig. 8 AUC and success rate curves illustrate cumulative percentage of landslide occurrences (*y-axis*) in landslide susceptibility index rank (*x-axis*)
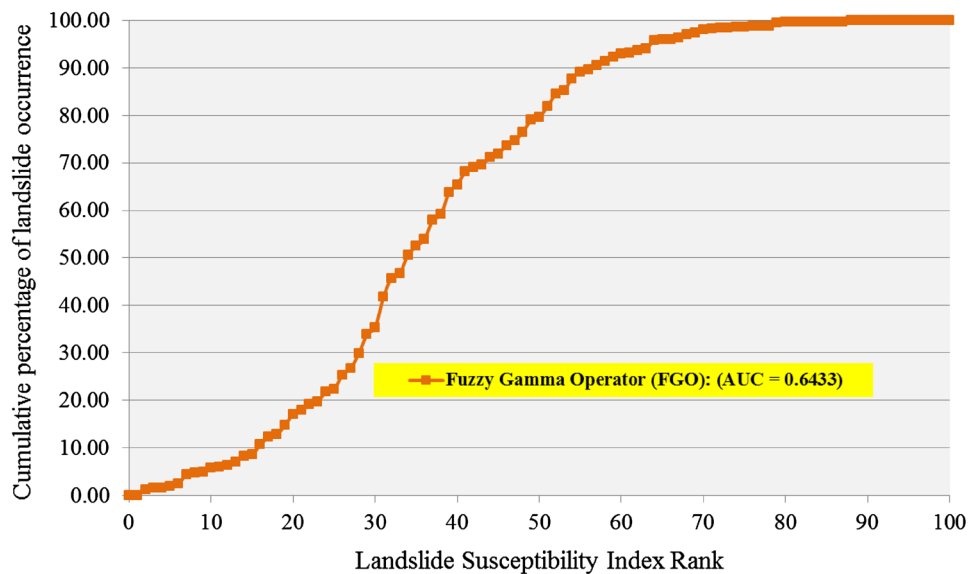
susceptibility zonation for the study area was prepared on the basis of Fuzzy Gamma Operator model. In the present study, fuzzy operator value was integrated by combining eight causative factors such as slope gradient, slope aspect, curvature, elevation, land use and land cover, drainage density, lineament density and topographical wetness index with the inventory. The landslide susceptibility index maps produced by the fuzzy product and fuzzy γ operator with γ

values was validated using success rate accuracy, i.e., AUC of 64.33% and R-Index which indicated the consistency of landslide susceptibility classes. This study will be helpful for carry out risk assessment, risk reduction and mitigation in the near future. Hence, this landslide susceptibility map is valuable resource to delineate landslide prone areas, and key source of valuable information to policy makers, planners, geologists, and civil engineers which provides the

512
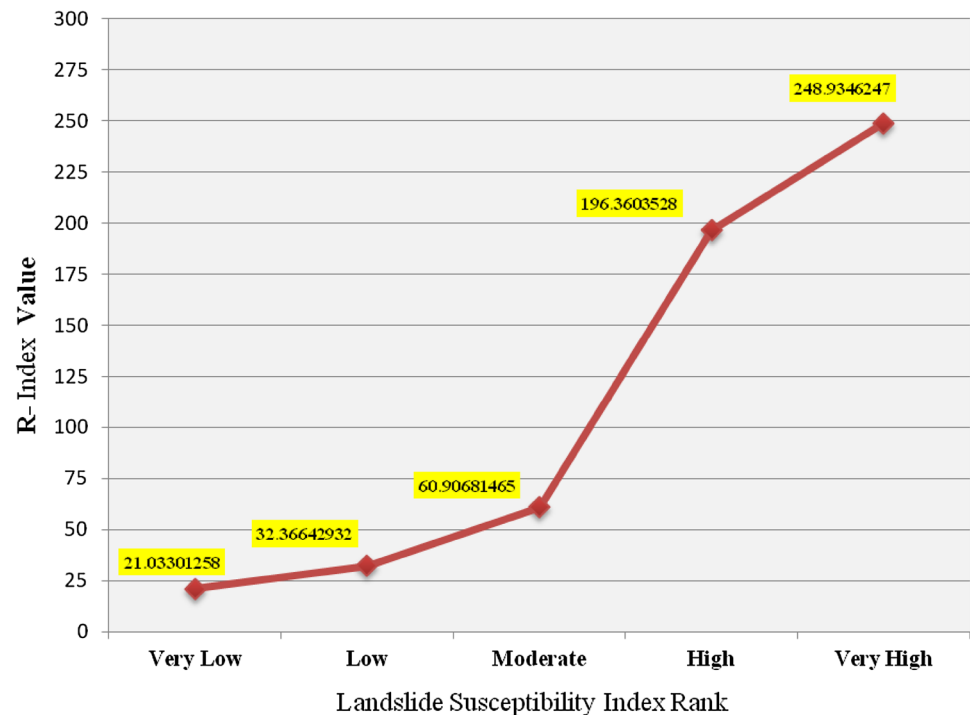
Model. Earth Syst. Environ. (2017) 3:499–514

Fig. 9 R-index and success
rate curves illustrate cumulative
percentage of landslide occur-
rences (*y-axis*) in landslide sus-
ceptibility index rank (*x-axis*)

necessary information to set up early warning systems or
to develop possible measures to safeguard human life and
property in the study area.

References

Aier I (2005) Landslides along the Kohima-Dimapur Road: Their
Causes and Possible Remedial Measures. Unpublished Ph. D.
Thesis, Department of Geology, Nagaland University, Kohima

Akgün A, Bulut F (2007) GIS-based landslide susceptibility for
Arsin-Yomra (Trabzon, North Turkey) region. Environ Geol
51(8):1377–1387

Aleotti P, Chowdhury R (1999) Landslide hazard assessment: sum-
mary review and new perspectives. Bull Eng Geol Environ
58:21–44. doi:10.1007/s100640050066

Alexander D (1993) Natural disasters. Kluwer Academic Publishers,
Dordrecht. pp. 242–264, 374–390

Anbazhagan S, Ramesh V (2014) Landslide hazard zonation mapping
in ghat road section of Kolli hills, India. J Mt Sci 11(5):1308–
1325. doi:10.1007/s11629-012-2618-9

Ayalew L, Yamagishi H, Marui H et al (2005) Landslides in Sado
Island of Japan: part II. GIS-based susceptibility mapping with
comparisons of results from two methods and verifications. Eng
Geol 81(4):432–445. doi:10.1016/j.enggeo.2005.08.004

Balamurugan G, Ramasamy SM (2006) Tectonic grains and slope
with special reference to landslide in Palani to Kodaikanal

Ghat road using remote sensing and GIS techniques. In: Basa-
varaiappa et al (ed) Remote sensing and GIS applications, Bel-
lur Prakashana, Mysore, pp 96–102.

Balamurugan G, Ramesh V, Touthang M (2016) Landslide sus-
ceptibility zonation mapping using frequency ratio and fuzzy
gamma operator models in part of NH-39, Manipur, India. Nat
Hazards. doi:10.1007/s11069-016-2434-6

Barredo JI, Benavidesz A, Herhl J et al (2000) Comparing heuristic
landslide hazard assessment tech-niques using GIS in the Tira-
jana basin, Gran Canaria Is-land, Spain. Int J Appl Earth Obs
Geoinf 2(1):9–23

Begueria S (2006) Validation and evaluation of predictive mod-
els in hazard assessment and risk management. Nat Hazards
37:315–329. doi:10.1007/s11069-005-5182-6

Beven K, Kirkby MJ (1979) A physically based, variable con-
tributing area model of basin hydrology. Hydrol Process
15:1993–2011

Bonham-Carter GF (1994) Geographic information systems for
geoscientists: modelling with GIS. Elsevier Butterworth-
Heine-mann, Oxford, pp 292–302

Carrara A (1988) Landslide hazard mapping by statistical
methods:a black box model approach. In: Proc of the Work-
shop on Natural Disaster in European Mediterranean Coun-
tries. Perugia, Italy. Consiglio Nazionale delle Ricerche.

Champati Ray PK, Dimri S, Lakhera RC et al (2007) Fuzzy-
based method for landslide hazard assessment in active seis-
mic zone of Himalaya. Landslides 4:101–111. doi:10.1007/
s10346-006-0068-6

Corominas J, Moya J (2008) A review of assessing landslide fre-
quency for hazard zoning purposes. Eng Geol 102:193–213.
doi:10.1016/j.enggeo.2008.03.018

Dai FC, Lee CF (2001) Frequency–volume relation and prediction
of rainfall-induced landslides. Eng Geol 59:253–266

Dai FC, Lee CF, Ngai YY (2002) Landslide risk assessment and management: an overview. Eng Geol 64(1):65–87. doi:10.1016/S0013-7952(01)00093-X

Das I, Stein A, Kerle N et al (2012) Landslide susceptibility mapping along road corridors in the Indian Himalayas using Bayesian logistic regression models. Geomorphology 179:116–125

Devoli G, Morales A, Hoeg K (2007) Historical landslides in Nicaragua—collection and analysis of data. Landslides 4(1):518. doi:10.1007/s10346-006-0048-x.

Directorate of Geology Mining (DGM) (2009) Geological Hazard Studies of Six District Headquarter Townships—Dimapur, Kohima, Wokha, Mokokchung, Zunheboto and Phek. Project Report on Zunheboto Town, Order No. /Geo-Hazards/Studies/2008/832–25, Dated- 28/03/09. Dimapur, pp 117–121

Duman TY, Can T, Gokceoglu C et al (2006) Application of logistic regression for landslide susceptibility zoning of Cekmece Area, Istanbul. Turkey. Environ Geol 51:241–256

Dussauge C, Helmstetter A, Grasso J-R et al (2002) Probabilistic approach to rock fall hazard assessment: potential of historical data analysis. Natural Hazards Earth Syst Sci 2:1–13

Dussauge C, Grasso J-R, Helmstetter A (2003) Statistical analysis of rockfall volume distributions: implications for rockfall dynamics. J Geophys Res 108(B6):2286. doi:10.1029/2001JB000650

Ehret D, Rohn J, Dumperth C et al (2010) Frequency ratio analysis of mass movements in the Xiangxi catchment, Three Gorges reservoir area, China. J Earth Sci 21(6):824–834. doi:10.1007/s12583-010-0134-9

Ercanoglu M, Gokceoglu C (2004) Use of fuzzy relations to produce landslide susceptibility map of a landslide prone area (West Black Sea Region, Turkey). Eng Geol 75:229–250. doi:10.1016/j.enggeo.2004.06.001

Fernandez Merodo JA, Pastor M, Mira P (2004) Modeling of diffuse failure mechanisms of catastrophic landslides. Comput Methods Appl Mech Eng 193:2911–2939. doi:10.1016/j.cma.2003.09.016

Geological Survey of India (GSI) (2001) Geology and mineral map of Manipur. Ministry of Mines, Government of India

Guzetti F, Carrara A, Andcardinali M et al (1999) Landslide hazard evaluation: a review of current techniques and their application in a multi-scale study, central Italy. Geomorphology 31:181–216. doi:10.1016/S0169-555X(99)00078-1

Guzzetti F, Malamud BD, Turcotte DL et al (2002) Power-law correlations of landslide areas in central Italy. Earth Planet Sci Lett 195:169–183

Guzzetti F, Mondini AC, Cardinali M et al (2012) Landslide inventory maps: new tools for an old problem. Earth Sci Rev 112:42–66

Husain Z (2008) Landslides hazards in the Sikkim Himalaya. In: Singh S et.al (eds) Environmental changes and geomorphic hazards, Bookwell, New Delhi. pp 113–120

Intarawichian N, Dasananda S (2011) Frequency ratio model based landslide susceptibility mapping in lower Mae Chaem watershed, Northern Thailand. Environ Earth Sci 64(8):2271–2285. doi:10.1007/s12665-011-1055-3

Jade S, Sarkar S (1993) Statistical Models for Slope Instability Classification. Eng Geol 36:91–98

Jenks GF (1967) The data model concept in statistical mapping. Int Year Book Cartogr 7:186–190

Kannan M, Saranathan E, Anabalagan R (2013) Landslide vulnerability mapping using frequency ratio model: a geospatial approach in Bodi-Bodimettu Ghat section, Theni district, Tamil Nadu, India. Arab J Geosci 6(8):2901–2913. doi:10.1007/s12517-012-0587-5

Kanungo DP, Arora MK, Sarkar S et al (2006) A comparative study of conventional, ANN black box, fuzzy and combined neural and fuzzy weighting procedures for landslide susceptibility zonation in Darjeeling Himalayas. Eng Geol 85:347–366. doi:10.1016/j.enggeo.2006.03.004

Kanungo DP, Arora MK, Sarkar S et al (2009) A fuzzy set based approach for integration of thematic maps for landslide susceptibility zonation. Georisk 3(1):30–43. doi:10.1080/17499510802541417

Lee S (2007) Application and verification of fuzzy algebraic operators to landslide susceptibility mapping. Environ Geol 52:615–623. doi:10.1007/s00254-006-0491-y

Lee S, Pradhan B (2006) Probabilistic landslide hazards and risk mapping on Penang Island, Malaysia. J Earth Syst Sci 115(6):661–672. doi:10.1007/s12040-006-0004-0

Lee S, Choi J, Min K (2002) Landslide susceptibility analysis and verification using the Bayesian probability model. Environ Geol 43:120–131. doi:10.1007/s00254-002-0616-x

MWR Ministry of Water Resources (2013) Ground Water Information Booklet Kohima District, Nagaland. Guwahati

Nagarajan R, Roy A, Kumar RV et al (2000) Landslide hazard susceptibility mapping based on terrain and climatic factors for tropical monsoon regions. Bull Eng Geol Environ 58:275–287. doi:10.1007/s002540050348

Nandi A, Shakoor A (2008) Application of logistic regression model for slope instability prediction in Cuyahoga River Watershed, Ohio, USA. Georisk 2(1):16–27. doi:10.1080/17499510701842221.

Nandi A, Shakoor A (2010) A GIS-based landslide susceptibility evaluation using bivariate and multivariate statistical analyses. Eng Geol 110(1–2):11–20

Naveen Raj T, Ram Mohan V, Backiaraj S et al (2011) Landslide Hazard Zonation Using the Relative Effect method In South Eastern Part Of Nilgiris, Tamilnadu, India. Int J Eng Sci Technol (IJEST) 3(4):3260–3265

Pachauri AK, Gupta PV, Chander R (1998) Landslide zoning in a part of the Garhwal Himalayas. Environ Geol 36:325–334. doi:10.1007/s100649900032

Parise M (2001) Landslide mapping techniques and their use in the assessment of the landslide hazard. Phys Chem Earth (C) 26:697–703

Pattusamy S, Purusothaman BM (2014) Disaster management and mapping using remote sensing and GIS. J Comput Biosci Eng 1(3)

Pradhan B, Lee S (2010) Delineation of landslide hazard areas on Penang Island, Malaysia, by using frequency ratio, logistic regression, and artificial neural network models. Environ Earth Sci 60:1037–1054. doi:10.1007/s12665-009-0245-8

Pradhan B, Lee S, Buchroithner MF (2009) Use of geospatial data and fuzzy algebraic operators to landslide-hazard mapping. Appl Geomat 1:3–15. doi:10.1007/s12518-009-0001-5

Ramesh V, Anbazhagan S (2015) Landslide susceptibility mapping along Kolli hills Ghat road section (India) using frequency ratio, relative effect and fuzzy logic models. Environ Earth Sci 73(12):8009–8021. doi:10.1007/s12665-014-3954-6

Ray Champati PK, Dimri S, Lakhera RC et al (2007) Fuzzy-based method for landslide hazard assessment in active seismic zone of Himalaya. Landslides 4:101–111

Regmi NR, Giardino JR, McDonald EV et al (2014) A comparison of logistic regression-based models of susceptibility to landslides in western Colorado, USA. Landslides 11:247–262. doi:10.1007/s10346012-0380-2.

Kumar R, Anbalagan R (2015) Landslide susceptibility zonation in part of Tehri reservoir region using frequency ratio, fuzzy logic and GIS. J Earth Syst Sci 124(2):431–448

Saha AK, Gupta RP, Sarkar I et al (2005) An Approach for GIS-based statistical landslide susceptibility zonation—with a case Study in the Himalayas. Landslides 2:61–69

Sasaki Y, Abe M, Hirano I (1991) Fractals of slope failure size-number distribution. J Jpn Soc Eng Geol 32:1–11

514

Model. Earth Syst. Environ. (2017) 3:499–514

Shirzadi A, Saro L, Joo OH et al (2012) A GIS-based logistic regression model in rock-fall susceptibility mapping along a mountainous road: salavat Abad case study, Kurdistan, Iran. Nat Hazards 64:1639–1656

Srivastava V, Srivastava H, Lakhera RC (2010) Fuzzy gamma based geomatic modeling for landslide hazard susceptibility in a part of Tons river valley, northwest Himalaya, India. Geomat Nat Hazards Risk 1(3):225–242

Sujatha ER, Kumaravel P, Rajamanickam GV (2011) GIS based landslide susceptibility mapping of Tevankarai Ar sub-watershed, Kodaikkanal, India using binary logistic regression analysis. J Mt Sci 8:505–517. doi:10.1007/s11629-011-2157-9

Sujatha ER, Rajamanickam V, Kumaravel P et al (2013) Landslide susceptibility analysis using probabilistic likelihood ratio model—a geospatial-based study. Arab J Geosci 6:429–440. doi:10.1007/s12517-011-0356-x

Supongtemjen (2006) Geological investigation of land instability between Kohima and Zhadima. Unpublished Ph. D. Thesis, Department of Geology, Nagaland University, Kohima

Tangestani MH (2004) Landslide susceptibility mapping using the fuzzy gamma approach in a GIS, Kakan catchment area, southwest Iran. Aust J Earth Sci 51(3):439–450

Thong GT, Thingo V, Walling T (2006). Geotechnical Investigations of Land Instability in Kohima Town and along NH 39, between Chumukedima and Kohima. Project Report of ISRO Project. No. 10/4/415, 2002, Kohima

Tunusluoglu MC, Gokceoglu C, Nefeslioglu HA, Sonmez H (2008) Extraction of potential debris source areas by logistic regression technique: a case study from Barla, Besparmak and Kapi mountains (NW Taurids, Turkey). Environ Geol 54(1):9–22

Van Westen CJ (1997) Statistical Landslide Hazard Analysis. In: Application Guide, ILWIS 2.1 for WindowsITC, Enschede, The Netherlands, pp 73–84

Van Westen CJ, Terlien MTJ (1996) An approach towards deterministic landslide hazard analysis in GIS. A case study from Manizales (Colombia). Earth Surf Processes Landf 21(9):853–868

Varnes DJ (1984) Landslide hazard zonation: a review of principles and practice. UNESCO, Paris, pp 1–63

Walling T (2005) Geological investigation of land instability in Kohima Town, Nagaland. Unpublished PhD thesis, Nagaland University, Kohima

Xu C, Xu X, Dai F et al (2013) Application of an incomplete landslide inventory, logistic regression model and its validation for landslide susceptibility mapping related to the May 12, 2008 Wenchuan earthquake of China. Nat Hazards 68:883–900. doi:10.1007/s11069-0130661-7

Yilmaz I, Keskin I (2009) GIS based statistical and physical approaches to landslide susceptibility mapping (Sebinkarahisar, Turkey). Bull Eng Geol Environ 68:459–471. doi:10.1007/s10064-009-0188-z

Yilmaz I, Marschalko M, Bednarik M (2012) Comments on, Landslide susceptibility zonation study using remote sensing and GIS technology in the Ken-Betwa River Link area, India, by Avtar, R., Singh, C.K., Singh, G., Verma, R.L., Mukherjee, S., Sawada, H., in Bulletin of Engineering Geology and the Environment. pp 803–804. Bull Eng Geol Environ 71:803–805. doi:10.1007/s10064-011-0406-3

Yin KL, Yan TZ (1988) Statistical prediction model for slope instability of metamorphosed rocks. In: Proceedings of the 5th international symposium on landslides, vol 2. Lausanne, pp 1269–1272.

Zadeh LA (1965) Fuzzy sets information and control. Inf control 8:338–353

Zimmermann HJ (1996) Fuzzy set theory and it applications. Kluwer Academic Publishers, Norwell p 435